

AFTERGLOW EMISSION FROM NAKED GAMMA-RAY BURSTS

PAWAN KUMAR

Institute for Advanced Study, Princeton, NJ 08540; pk@ias.edu

AND

ALIN PANAITESCU

Department of Astrophysical Sciences, Princeton University, NJ 08544; adp@astro.princeton.edu

Received 2000 June 21; accepted 2000 August 8; published 2000 September 19

ABSTRACT

We calculate the *afterglow* emission for gamma-ray bursts (GRBs) going off in an extremely low density medium, referred to as *naked bursts*. Our results also apply to the case where the external medium density falls off sharply at some distance from the burst. The observed afterglow flux in this case originates at high latitudes, i.e., where the angle between the fluid velocity and the observer line of sight is greater than Γ^{-1} . The observed peak frequency of the spectrum for naked bursts decreases with observer time as t^{-1} , and the flux at the peak of the spectrum falls off as t^{-2} . The 2–10 keV X-ray flux from a naked burst of average fluence should be observable by the *Swift* satellite for time duration of about 10^3 longer than the burst variability timescale. The high-latitude emission contributes to the early X-ray afterglow flux for any GRB, not just naked bursts, and can be separated from the shocked interstellar medium emission by their different spectral and temporal properties. Measurements of the high-latitude emission could be used to map the angular structure of GRB-producing shells.

Subject headings: gamma rays: bursts — gamma rays: theory

1. INTRODUCTION

A majority of long-duration gamma-ray bursts (GRBs; lasting 10 s or more) detected by the Dutch-Italian satellite *BeppoSAX* have detectable X-ray afterglows. The afterglow properties of shorter duration bursts is unknown, and it is possible that these bursts go off far away from galactic centers, where the interstellar medium (ISM) density is low. Will such bursts produce observable afterglows?

The purpose of this Letter is to show that all bursts, irrespective of the ISM density, should have a detectable afterglow emission. During the GRB the radiation is received from a region of the fireball of angular size Γ^{-1} along the line of sight to the center of the explosion. Emission from higher latitudes, $\theta > \Gamma^{-1}$, is received over a time interval that is long compared to the duration of the burst and, although this radiation is relativistically beamed away from the observer, it nevertheless has significant magnitude. We calculate this emission and apply it to GRBs going off in a very low density ISM (§ 2). We also consider a case where the density of the circumburst medium drops off abruptly at some radius (§ 3).

2. HIGH-LATITUDE EMISSION FROM A RELATIVISTIC SHELL

Consider a spherical shell moving with Lorentz factor Γ . The shell is shock-heated at some initial time and starts to radiate. The emissivity in fluid rest frame ϵ'_ν is a function of shell radius r , and we assume that it is independent of the angle θ relative to the observer's line of sight toward the center of the shell. We also assume that as a result of the radiative electron cooling and the adiabatic expansion of the shell (or some other process) the emissivity in the observed energy band drops to zero when the shell radius is r_c . One can show in this case that the observed peak flux at observer time $t \gg r_c/\Gamma^2$ decreases as t^{-2} and that the observed peak frequency decreases as t^{-1} .

A simple physical explanation for these results is the following. The flux per unit frequency from a relativistic source moving at an angle $\theta \gg \Gamma^{-1}$ is smaller by a factor of $(\theta\Gamma)^6$ compared to the case where the source is moving directly to-

ward the observer (assume a flat spectrum for simplicity). Integrating over sources located on equal arrival time surface, we find the flux ratio to be $(\theta\Gamma)^4$. The emission from angle θ arrives at a time that is larger than the photon arrival time from a source at $\theta = 0$ by a factor of $(\theta\Gamma)^2$. Thus, the observer sees the flux falling off as t^{-2} . The observed frequency ratio in the two cases, for a fixed source frequency, is $(\theta\Gamma)^{-2} \propto t^{-1}$. A derivation for a more general case is given below.

The flux received at frequency ν from a shell moving with Lorentz factor Γ and velocity v is given by

$$f_\nu(t) = \frac{1}{4\pi d^2} \int d^3r \frac{\epsilon'_\nu(\mathbf{r}, t_{\text{lab}})}{\Gamma^2(1 - v\mu)^2}, \quad (1)$$

where $\mu = \cos \theta$, θ is the angle between fluid velocity and the line of sight to the observer, and $\nu' = \nu\Gamma(1 - v\mu)$ and ϵ'_ν are the frequency and emissivity in the shell rest frame at radius r and laboratory frame time $t_{\text{lab}} = t_+ r\mu$. For a shell of thickness Δr (in the lab frame) much smaller than r , the angular integration in the above equation can be carried out to yield

$$f_\nu = \frac{1}{2d^2} \int dr r \frac{\Delta r \epsilon'_\nu(r)}{\Gamma^2(1 - v\tilde{\mu})^2}, \quad (2)$$

where $\tilde{\mu}(r) = (t_{\text{lab}} - t)/r(t_{\text{lab}})$.

Let us assume that the observed spectrum during the GRB phase, i.e., before the shell cools, is a power-law function of index β between the observed energy band and the peak of the spectrum, $\epsilon'_\nu = \epsilon'_\nu{}^\beta$, and that, as θ is varied, the comoving frame observing frequency does not pass through any breaks. In this case we can rewrite equation (2) as

$$f_\nu = \frac{\nu^\beta}{2d^2} \int dr \frac{\Delta r \epsilon'_\nu r^{3-\beta}}{[\Gamma(t + r/v - t_{\text{lab}})]^{2-\beta}}. \quad (3)$$

As mentioned above, we consider the case where the injection of accelerated electrons stops at a certain radius r_c . This

can happen either because the internal shock has finished traversing the shell or because the density of the ISM drops by a large factor. In both cases the electrons undergo adiabatic cooling beyond r_c , which leads to a sharp falloff of ϵ' (see § 3); for radiative electrons ϵ' drops off even faster.

The integrand in equation (3) is a rapidly increasing function of r ; hence, most of the contribution comes from $r \sim r_c$ and the peak flux is given by

$$f_{\nu_p}(t) \approx f_{\nu_p}(t_c) \left(\frac{2\tau}{t + \tau - t_c} \right)^2, \quad \tau \equiv \frac{r_c}{2\Gamma_c^2}, \quad (4)$$

where $t_c = t(r_c)$ and $\Gamma_c \equiv \Gamma(r_c)$. The peak frequency ν_p of the observed flux decreases with time as

$$\nu_p(t) = \nu_p(t_c) \left(\frac{\tau}{t + \tau - t_c} \right). \quad (5)$$

For a shell that is energized by the collision with another shell (i.e., internal shocks) and expands in a vacuum, τ is also a measure of the duration δt of the pulse emitted by the shell. For $t \gg t_c$, equations (4) and (5) become

$$f_{\nu_p}(t) = f_{\nu_{p,c}} \left(\frac{\delta t}{t} \right)^2, \quad \nu_p(t) = \nu_{p,c} \left(\frac{\delta t}{t} \right). \quad (6)$$

where $f_{\nu_{p,c}} \equiv f_{\nu_p}(t_c)$ and $\nu_{p,c} \equiv \nu_p(t_c)$. For power-law spectra, the observed flux at a frequency ν can be calculated from equations (3) and (6):

$$f_{\nu}(t) = f_{\nu_{p,c}} \left(\frac{\delta t}{t} \right)^{2-\beta} \left(\frac{\nu}{\nu_{p,c}} \right)^{\beta}. \quad (7)$$

For a collimated explosion of opening angle θ_0 , the flux f_{ν} drops off rapidly to zero for $t > \delta t(\Gamma\theta_0)^2$.

For a GRB consisting of N pulses, the high-latitude afterglow flux is the sum of flux from each pulse given in equation (7). For an average peak amplitude of $f_{\nu_{p,c}}$, the afterglow flux is approximately equal to $f_{\nu_{p,c}} N^{\beta-1} (t_G/t)^{2-\beta}$, where $t_G \sim N\delta t$ is the duration of the GRB.

The low-energy power-law index for GRBs is in the range between -1 and 2 with the peak of the distribution at ~ 0 , and the high-energy index is between -3 and -0.3 with the peak at -1.2 (Preece et al. 2000). Thus, the low-energy light curve for naked bursts is expected to fall off as t^{-2} , whereas the light curve at high energy should decline as $t^{-3.2}$. For synchrotron emission, the spectral index below the peak is $\beta = \frac{1}{3}$ and the afterglow from high-latitude emission is expected to decline like $t^{-5/3}$ until the synchrotron peak passes through the observing band.

As an example, consider a naked GRB lasting for 10 s and with a mean flux of 10^{-6} ergs cm^{-2} s^{-1} and the spectral peak at a few hundred keV. At 10^3 s after the burst, the spectral peak is in the 2–10 keV band and the flux is $\sim 10^{-12}$ ergs cm^{-2} s^{-1} (see Fig. 1). Assuming that the optical emission is not self-absorbed, the optical flux at $t = 300$ s corresponds to $R \sim 25$.

The high-latitude emission should be detectable by the *Swift* satellite as an X-ray afterglow following short-duration GRBs, which are perhaps produced as a result of a neutron star merger in a low-density medium. Some of the early X-ray afterglows observed by *BeppoSAX* have a power-law decay index of ≥ 1.6 ,

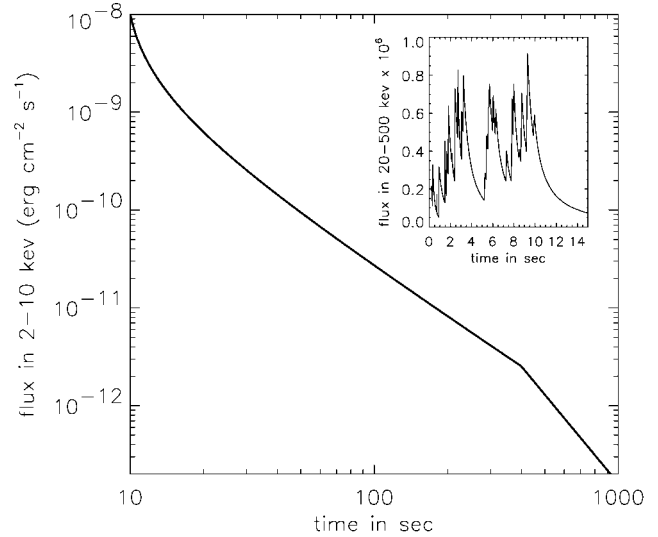


FIG. 1.—2–10 keV light curve arising from high latitudes, i.e., $\theta > \Gamma^{-1}$. The ISM density is assumed to be zero. The peak flux for the GRB is taken to be 10^{-12} ergs cm^{-2} s^{-1} eV^{-1} ; the burst duration is 10 s, the low-energy slope of the spectrum (β) is $\frac{1}{3}$, and the high-energy index is -1 . The burst duration and the peak flux set the x- and y-axis scales, and the spectral slopes set the power-law decline of the light curve (see text). The power-law index of the light curve is $5/3$ for $t < 400$ s and steepens to 3 when the peak frequency passes through the X-ray band. The inset shows the GRB light curve in the 20–500 keV band; the mean pulse width is 0.4 s.

which could have had a contribution from the high-latitude emission. In the few cases where an X-ray afterglow was continuously monitored for 10^3 – 10^4 s after the main burst (i.e., GRB 910402: Tkachenko et al. 2000; GRB 920723: Burenin et al. 1999; GRB 980923: Giblin et al. 1999), the X-ray light curve exhibited a decay significantly slower than what is expected from the high-latitude emission, implying that the emission from the external shock must have been dominant from very early times.

The ratio of the observed flux from the shocked ISM gas and the high-latitude emission (Q) depends on burst parameters and, generally, on the density of the ISM. An important time-scale for this comparison is the shell deceleration time $t_{\text{da}} \approx 100 E_{52}^{1/3} (1 - \eta)^{1/3} (\eta n_0 \Gamma_2^8)^{-1/3}$ s, where E_{52} is the isotropic equivalent of energy in observed gamma-ray emission in units of 10^{52} ergs, $\Gamma_2 = \Gamma_0/100$, Γ_0 is the initial Lorentz factor of ejecta, and η is the efficiency factor for converting energy in the explosion to the observed gamma-ray emission. We consider t_{da} less than or greater than the GRB duration t_G separately below.

Let us first consider $t_{\text{da}} \leq t_G$. For an ISM density (n_0) larger than 10^{-2} cm^{-3} and for fractional energy in the magnetic field $\epsilon_B \sim 10^{-2}$, the soft X-ray domain is above the cooling frequency after the GRB, and in this case Q is independent of n_0 . For an electron energy index $p = 2$, $Q \sim 0.3 (\nu_G/\nu)^{\beta+1} \epsilon_e (t/\delta t_G)^{1-\beta} (1 - \eta)\eta^{-1}$, where ν_G is the observed peak of the GRB spectrum, ν is the frequency for the afterglow observation, and ϵ_e is the energy fraction in electrons in external shock. For $\nu_G/\nu = 20$, $\epsilon_e = 0.1$, $\beta = 0$, and $\eta = 0.1$, the emission from the external shock is larger by about a factor of 5 at the end of the GRB. This result has a weak dependence on p .

For $t_{\text{da}} \gg t_G$, as is expected for low-density ISM, and the observing frequency smaller than the cooling frequency, and for $p = 2$ and $\beta = 1$, we find $Q \approx 8 \epsilon_B^{3/2} \epsilon_e E_{52}^{1/4} n_0^{1/2} t_{\text{da}}^{1/4} \times$

$(\nu_G/\nu)^2 \nu_{10}^{1/2} (1-\eta)^{5/4} \eta^{-5/4}$; ν_{10} is frequency in units of 10 keV. As an example, for $\epsilon_e = 0.1$, $\epsilon_B = 10^{-2}$, $\eta = 0.1$, $\nu_G/\nu = 20$, $\nu_{10} = 1$, $E_{52} = 1$, and $t_{\text{da}} = 100$ s, the two emissions are equal at the deceleration time for $n \sim 4 \times 10^{-3} \text{ cm}^{-3}$. For $t_{\text{da}} \gg t_G$, ν greater than the cooling frequency, and $\beta = 1$, $Q = 2\epsilon_e(t/t_{\text{da}})^3 (\nu_G/\nu)^2 (1-\eta)\eta^{-1}$.

One should be able to separate out the contributions of the high-latitude and shocked gas emissions by using the difference in their spectra and light-curve slopes: the X-ray spectra for shocked low-density ISM is $f_\nu \propto t^{-3(p-1)/4} \nu^{-(p-1)/2}$, whereas the high- θ spectrum is the low-energy part of the GRB spectrum, i.e., $f_\nu \propto t^{-(2-\beta)} \nu^\beta$ with $-1 < \beta < 2$.

3. FIREBALL EXPANSION INTO AN ISM WITH A DENSITY DISCONTINUITY

In this section we consider an external shock propagating in an ISM that consists of two regions of different densities. The model we consider consists of a fireball that shocks the ISM, producing a standard afterglow emission, and then at some radius r_{ad} the density of the medium drops precipitously and the shell expands adiabatically so that the thermal energy of the protons, electrons, and magnetic field is converted back to the bulk kinetic energy of the shell. We follow the shell evolution and synchrotron radiation starting from the time of the free expansion of the shell.

The thermal Lorentz factor of particles, in an adiabatically expanding shell, decreases as $\gamma_{\text{th}} \propto V^{-1/3}$, and the bulk Lorentz factor of the shell (Γ) increases with time as $V^{1/3}$, where $V = \pi\theta_0^2 r^2 \Delta r$ is the comoving volume of the shell and $\Delta r \propto r^{1/4}$ is the comoving shell thickness.

We consider the collimation angle θ_0 of the ejecta to be constant, in which case the thermal Lorentz factor decreases with r as $r^{-3/4}$ and the bulk Lorentz factor of the shell increases as $r^{3/4}$. Therefore, the evolution of the thermal Lorentz factor is given by

$$\gamma_{\text{th}} \approx \Gamma_{\text{ad}} \left(\frac{9}{8} - \frac{t}{8t_{\text{ad}}} \right)^{3/2}, \quad (8)$$

where Γ_{ad} and t_{ad} are the bulk Lorentz factor and the observer time, respectively, at the onset of the free adiabatic expansion. The bulk Lorentz factor $\Gamma \approx \Gamma_{\text{ad}}^2/\gamma_{\text{th}}$.

The magnetic field strength, assuming that it is tangled, decreases as $V^{-2/3} \propto \gamma_{\text{th}}^2$. Thus, the peak synchrotron frequency, in the observer frame, scales as γ_{th}^3 , and the peak flux $f_{\nu_p} \propto \gamma_{\text{th}}$. The flux at a frequency greater than the synchrotron peak ν_m but smaller than the cooling frequency ν_c is given by

$$f_\nu \propto \left(\frac{9}{8} - \frac{t}{8t_{\text{ad}}} \right)^{3(3p-1)/4}, \quad (9)$$

and the power-law index $\alpha = -d \ln f_\nu / d \ln t$ is

$$\alpha = \frac{3(3p-1)(t/t_{\text{ad}})}{4(9-t/t_{\text{ad}})}. \quad (10)$$

Therefore, the afterglow light curve steepens continuously; in the beginning of the adiabatic expansion $\alpha = 3(p-1)/4$, while at $t = 3t_{\text{ad}}$, $\alpha = 3(3p-1)/8$, assuming that $\nu_m < \nu < \nu_c$. As the light-curve slope increases with time, the flux from higher latitudes takes over. For a shell interacting with a uni-

form circumburst material at $r < r_{\text{ad}}$, $\Gamma \propto r^{-3/2}$, and thus $t_{\text{ad}} = r_{\text{ad}}/8\Gamma_{\text{ad}}^2$. For $t \gg t_{\text{ad}}$ equation (4) gives

$$f_\nu(t) = 16f_{\nu_{p,\text{ad}}} \left(\frac{t_{\text{ad}}}{t} \right)^{2-\beta} \left(\frac{\nu}{\nu_{p,\text{ad}}} \right)^\beta; \quad (11)$$

therefore, the high-latitude emission prevents α from becoming larger than $(p+3)/2$.

These results apply over a limited range of t . At late times the nonzero density of the ISM prevents the free expansion of the shell and the freshly shock-heated gas contributes to the observed flux. The free expansion of the shell is terminated when the mass of the swept-up low-density gas is $\sim E/\Gamma_{\text{ad}}^2$, E being the energy of the adiabatic shell. Thus, the radius at which the free adiabatic expansion is terminated is $r/r_{\text{ad}} \sim (n_1/n_2)^{2/9}$, where n_1 and n_2 are the densities of the high- and low-density ISM, respectively. The time in the observer frame when the adiabatic expansion ends is

$$\frac{t_f}{t_{\text{ad}}} \approx 9 - 8 \left(\frac{n_2}{n_1} \right)^{1/9}. \quad (12)$$

For $n_2/n_1 = 0.1$ (0.01), free expansion is terminated at $t_f/t_{\text{ad}} = 2.8$ (4.2).

The value of α reverts back to $3(p-1)/4$ when the emission from the shocked low-density ISM takes over. At the time when the adiabatic expansion of the shell ends, the ratio of the flux from the low-density shocked gas to the flux at t_{ad} is $\sim (n_2/n_1)^{(7-p)/12}$. If the fractional energies in electrons ϵ_e and magnetic field ϵ_B are same for shocks in the high- and low-density ISM, then the flux at t_f due to high-latitude emission and the low-density shocked gas are approximately equal for $10^{-3} < n_2/n_1 < 10^{-1}$. Since the observed flux for frequency between ν_m and ν_c is proportional to $\epsilon_e^{(p-1)} \epsilon_B^{(p+1)/4}$, values of ϵ_e and ϵ_B for the shocked lower density medium smaller by a factor of 10 could reduce the flux from the low-density shock gas so that the high-latitude emission dominates for $\sim 20t_{\text{ad}}$, and during this period the power-law index of the light curve is $\alpha = (p+3)/2$; for $\nu > \nu_c$, $\alpha = (p+4)/2$.

The optical light curve of the afterglow of GRB 000301C fell off as $\sim t^{-1}$ for the first 3 days and subsequently steepened to $\sim t^{-3}$ (Rhoads & Fruchter 2000). From simultaneous optical-IR observations, Rhoads & Fruchter (2000) and Sagar et al. (2000) have found that $\beta = -0.9 \pm 0.1$ at $t \sim 4$ days. A possible explanation for the steep decay seen at late time in this afterglow is that the ISM density fell off at some radius¹ and the subsequently observed afterglow emission arose at $\theta \gg \Gamma^{-1}$, yielding a power-law decaying light curve of index $\alpha = 2 - \beta = 2.9 \pm 0.1$, which is consistent with the data.

Figure 2 shows the observed R -band data for GRB 000301C and the theoretically calculated light curve based on the model described here and in Panaitescu & Kumar (2000). The transition time for light-curve steepening is $\sim 10t_{\text{ad}}$, which is roughly consistent with the observations. It has been shown by Kumar & Panaitescu (2000) that the timescale for light-curve steepening due to jet edge effects in a homogeneous ISM is roughly comparable. The late-time power-law index according to the

¹ The optical emission of the afterglow of GRB 000301C shows considerable variability prior to the steepening of the light-curve decline. This suggests that there are significant fluctuations in the ISM density, and so it is not altogether surprising that the external medium density drops to a small value at some radius.

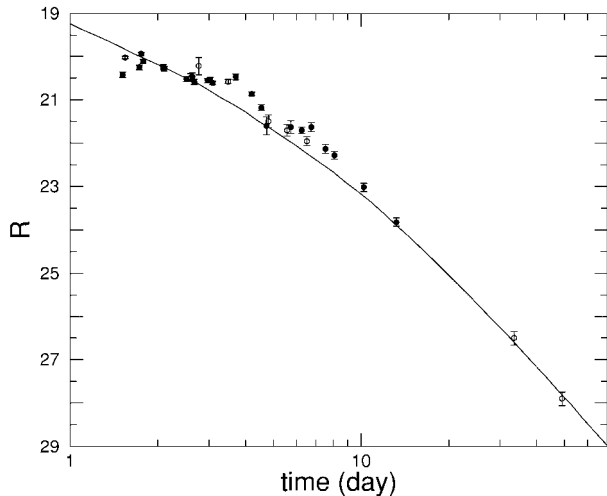


FIG. 2.— R -band light curve (solid line) from a spherical remnant running into a uniform density ISM that ends at some radius. Beyond this radius, at 3 days in the observer frame, the shell undergoes adiabatic expansion. Before the break the optical flux decay slope is $3(p-1)/4$, and after the break it is $(p+4)/2$ for frequencies above the cooling break. The parameters for the model are $E = 2 \times 10^{52} F$ ergs, $p = 2.6$, $n = F^{-1} \text{ cm}^{-3}$, $\epsilon_B = 5 \times 10^{-3} F^{1/3}$, and $\epsilon_e = 0.1 F^{-3/4}$, with the allowed value of F between 0.2 and 5. The cooling frequency crosses the R band around 5 days. The data for GRB 000301C are taken from Sagar et al. (2000), Massetti et al. (2000), and from GCN Circulars (Bernabei et al. 2000; Bhargavi & Cowsik 2000; Castro-Tirado et al. 2000; Fruchter et al. 2000a, 2000b, 2000c; Fynbo et al. 2000; Gal-Yam et al. 2000; Garnavich et al. 2000a, 2000b; Halpern et al. 2000a, 2000b, 2000c; Mujica et al. 2000; Veillet et al. 2000a, 2000b, 2000c, 2000d).

jet model is $\alpha = 1 - 2\beta = 2.8 \pm 0.2$ for adiabatic electrons radiating at optical frequencies, which is also consistent with the data. The different relationship between α and β in these two models can be used to distinguish between them.

4. CONCLUSIONS

The main conclusion of this work is that GRBs going off in a vacuum—*naked GRBs*—should have X-ray afterglow emission detectable by the X-ray telescope aboard the *Swift* satellite for about an hour after the GRB. This radiation originates at the high latitude, $\theta \gg \Gamma^{-1}$, part of the gamma-ray emission surface.

The flux in a fixed observer energy band below the peak falls off as $t^{-5/3}$, while the peak flux decreases as t^{-2} . The peak frequency of the observed flux falls off as t^{-1} .

For a burst going off in a nonzero density ISM the early afterglow flux, within the first hour, is the sum of emission from the high-latitude and shocked ISM. The two can be distinguished based on the differences between their spectral and temporal slopes; the X-ray spectrum for the shocked ISM is $\sim \nu^{-1}$, whereas for the high-latitude radiation the spectrum should be the same as the GRB spectrum at low energies, i.e., $\sim \nu^{0.3}$. The measurement of the high-latitude afterglow emission should help map the irregularities in the ejecta producing the GRB and their collimation before these are detected in the emission from the shocked ISM.

The radiation emitted from latitudes $\theta \geq \Gamma^{-1}$ sets an upper bound on the steepness of the flux decline; we expect the observed gamma-ray flux for each individual peak within the burst to fall off less rapidly than $t^{-(2-\beta)}$, where t is measured from the peak of the pulse and β is the spectral index ($f_\nu \propto \nu^\beta$). A more rapid flux decline would be an indication of either an extremely small jet opening angle or a very inhomogeneous shell, as in the model suggested by Kumar & Piran (2000).

Another straightforward consequence of the high-latitude emission is that the power-law decline for the afterglow light curve cannot be larger than about 3, even when the fireball expands into vacuum. The observed late-time power-law index for the light curve of GRB 000301C is about 3, which is larger by about 2 compared to the early-time index. This large and rapid steepening of the light curve could arise when the late-time light curve is dominated by emission from high latitudes. The time to complete 90% of the steepening of the light curve for the high-latitude model is smaller by a factor of ~ 2 than in the jet model. The relationship between the index α of the light-curve decay and the spectral index β ($f_\nu \propto t^{-\alpha} \nu^\beta$) in the high-latitude model is $\alpha = 2 - \beta$, whereas in the jet model the relationship is $\alpha = -2\beta + 1$ if the electrons radiating at the observing frequency are in the fast-cooling regime and $\alpha = -2\beta$ if these electrons are in the slow-cooling regime. These differences can be used to distinguish between the two models.

We thank Bohdan Paczyński and Tsvi Piran for useful discussions.

REFERENCES

- Bernabei, S., et al. 2000, GCN Circ. 599 (<http://gcn.gsfc.nasa.gov/gcn/gcn3/599.gcn3>)
- Bhargavi, S., & Cowsik, R. 2000, GCN Circ. 630 (<http://gcn.gsfc.nasa.gov/gcn/gcn3/630.gcn3>)
- Burenin, R., et al. 1999, A&AS, 138, 443
- Castro-Tirado, A., et al. 2000, GCN Circ. 579 (<http://gcn.gsfc.nasa.gov/gcn/gcn3/579.gcn3>)
- Fruchter, A., et al. 2000a, GCN Circ. 602 (<http://gcn.gsfc.nasa.gov/gcn/gcn3/602.gcn3>)
- . 2000b, GCN Circ. 627 (<http://gcn.gsfc.nasa.gov/gcn/gcn3/627.gcn3>)
- . 2000c, GCN Circ. 701 (<http://gcn.gsfc.nasa.gov/gcn/gcn3/701.gcn3>)
- Fynbo, J., et al. 2000, GCN Circ. 576 (<http://gcn.gsfc.nasa.gov/gcn/gcn3/576.gcn3>)
- Gal-Yam, A., et al. 2000, GCN Circ. 593 (<http://gcn.gsfc.nasa.gov/gcn/gcn3/593.gcn3>)
- Garnavich, P., et al. 2000a, GCN Circ. 573 (<http://gcn.gsfc.nasa.gov/gcn/gcn3/573.gcn3>)
- . 2000b, GCN Circ. 581 (<http://gcn.gsfc.nasa.gov/gcn/gcn3/581.gcn3>)
- Giblin, T., et al. 1999, ApJ, 524, L47
- Halpern, J., et al. 2000a, GCN Circ. 578 (<http://gcn.gsfc.nasa.gov/gcn/gcn3/578.gcn3>)
- Halpern, J., et al. 2000b, GCN Circ. 582 (<http://gcn.gsfc.nasa.gov/gcn/gcn3/582.gcn3>)
- . 2000c, GCN Circ. 604 (<http://gcn.gsfc.nasa.gov/gcn/gcn3/604.gcn3>)
- Kumar, P., & Panaitescu, A. 2000, ApJ, 541, L9
- Kumar, P., & Piran, T. 2000, ApJ, 535, 152
- Massetti, N., et al. 2000, A&A, submitted (astro-ph/0004186)
- Mujica, R., et al. 2000, GCN Circ. 597 (<http://gcn.gsfc.nasa.gov/gcn/gcn3/597.gcn3>)
- Panaitescu, A., & Kumar, P. 2000, ApJ, in press
- Preece, R. D., Briggs, M. S., Malozzi, R. S., Pendleton, G. N., Paciesas, W. S., & Band, D. L. 2000, ApJS, 126, 19
- Rhoads, J. E., & Fruchter, A. S. 2000, ApJ, submitted (astro-ph/0004057)
- Sagar, R., Mohan, V., Pandey, S. B., Pandey, A. K., & Castro-Tirado, A. J. 2000, Bull. Astron. Soc. India, submitted (astro-ph/0004223)
- Tkachenko, A., Terenkov, O., Sunyaev, R., Burenin, R., Barat, C., Dezalay, J.-P., & Vedrenne, G. 2000, A&A, submitted (astro-ph/0005293)
- Veillet, C., et al. 2000a, GCN Circ. 588 (<http://gcn.gsfc.nasa.gov/gcn/gcn3/588.gcn3>)
- . 2000b, GCN Circ. 598 (<http://gcn.gsfc.nasa.gov/gcn/gcn3/598.gcn3>)
- . 2000c, GCN Circ. 610 (<http://gcn.gsfc.nasa.gov/gcn/gcn3/610.gcn3>)
- . 2000d, GCN Circ. 611 (<http://gcn.gsfc.nasa.gov/gcn/gcn3/611.gcn3>)